Functional Collaboration between Different Cyclin-Dependent Kinase Inhibitors Suppresses Tumor Growth with Distinct Tissue Specificity

DAVID S. FRANKLIN,[1]† VIRGINIA L. GODFREY,[2] DEBORAH A. O'BRIEN,[1,3,5]
CHUXIA DENG,[6] AND YUE XIONG[1,4,5]*

Lineberger Comprehensive Cancer Center,[1] Department of Pathology and Laboratory Medicine,[2] Departments of Cell Biology and Anatomy and Pediatrics,[3] Department of Biochemistry and Biophysics,[4] and Program in Molecular Biology and Biotechnology,[5] University of North Carolina at Chapel Hill, Chapel Hill, North Carolina 27599-7295, and Laboratory of Biochemistry and Metabolism, National Institute of Diabetes, Digestive and Kidney Diseases, National Institutes of Health, Bethesda, Maryland 20892[6]

The presence of two families of seven distinct mammalian cyclin-dependent kinase (CDK) inhibitor genes is thought to mediate the complexity of connecting a variety of cellular processes to the cell cycle control pathway. The distinct pattern of tissue expression of CDK inhibitor genes suggests that they may function as tumor suppressors with different tissue specificities. To test this hypothesis, we have characterized two strains of double mutant mice lacking either $p18^{INK4c}$ and $p27^{KIP1}$ or $p18^{INK4c}$ and $p21^{CIP1/WAF1}$. Loss of both p18 and p27 function resulted in the spontaneous development by 3 months of age of at least eight different types of hyperplastic tissues and/or tumors in the pituitary, adrenals, thyroid, parathyroid, testes, pancreas, duodenum, and stomach. Six of these hyperplastic tissues and tumors were in endocrine organs, and several types of tumors routinely developed within the same animal, a phenotype reminiscent of that seen in combined human multiple endocrine neoplasia syndromes. The p18-p21 double null mice, on the other hand, developed pituitary adenomas, multifocal gastric neuroendocrine hyperplasia, and lung bronchioalveolar tumors later in life. G_1 CDK2 and CDK4 kinase activities were increased in both normal and neoplastic tissues derived from mice lacking individual CDK inhibitors and were synergistically stimulated by the simultaneous loss of two CDK inhibitors. This indicates that an increase in G_1 CDK kinase activity is a critical step during but is not sufficient for tumor growth. Our results suggest that functional collaborations between distinct CDK inhibitor genes are tissue specific and confer yet another level of regulation in cell growth control and tumor suppression.

More than a dozen tumor suppressor genes have been identified thus far by virtue of their genetic mutations in human cancers. Some appear to function in a specific cell type, such as BRCA1 and BRCA2 in breast and ovarian cancer, Smad4 (Dpc4), APC, and Smad2 in colon cancer, and Menin in type 1 multiple endocrine neoplasia (MEN1). Other tumor suppressors, notably p53 and Rb, are mutated in a wide range of tumor types, indicating a more general function in tumor suppression (21, 32, 36). Conceptually, genes that negatively regulate the growth-suppressing activity of either p53 or pRb may be proto-oncogenes, as exemplified by the observation that MDM2 (26) and cyclin D1 (20), negative regulators of p53 and pRb, respectively, are frequently activated in human cancers and promote tumor growth when targeted for transgenic expression in mouse mammary tissues (22, 35). Likewise, genes that function to activate or to retain the growth suppression activity of either p53 or pRb are candidate tumor suppressors (32, 33). Indeed, the ARF-INK4a locus, the second most frequently disrupted locus in human cancers next to p53 (17, 25), encodes two

separate proteins, ARF and $p16^{INK4a}$, that positively regulate p53 and Rb, respectively (33). The high frequency of genetic alterations and the often nonoverlapping mutational pattern among the genes within each of these two pathways have led to the notion that functional inactivation of both the p53 and pRb pathways may be necessary for the development of different types of cancer.

Two families of cyclin-dependent kinase (CDK) inhibitors, totaling seven genes, have been identified in mammalian cells. Their similar biochemical activity in blocking CDK enzymes and maintaining the growth-suppressive activity of Rb predict a tumor suppression function for CDK inhibitor genes, yet only the $p16^{INK4a}$ gene has been directly linked to tumor growth by genetic alterations found in human cancers (17, 25) and by the early development of spontaneous tumors in mice lacking p16 (31). Neither mutational analysis in human tumors nor phenotypic examination of genetically targeted mice lacking any of the other individual CDK inhibitor genes has provided strong evidence for a direct role for any of the other CDK inhibitors as tumor suppressors. Mice lacking $p21^{CIP1/WAF1}$ (6), $p27^{KIP1}$ (10, 19, 23), $p57^{KIP2}$ (40, 41), or $p18^{INK4c}$ (11) do not develop spontaneous tumors at an early age. However, potential tumor suppression functions were suggested by the observations that cells lacking p21 are defective in a DNA damage-induced, p53-mediated G_1 checkpoint (3, 6), that mice lacking either p18 or p27 slowly develop intermediate-lobe pituitary tumors later in life (10, 11, 19, 23), that p27 heterozygous mice have a

* Corresponding author. Mailing address: Lineberger Comprehensive Cancer Center, University of North Carolina, Chapel Hill, NC 27599-7295. Phone: (919) 962-2142. Fax: (919) 966-8799. E-mail: yxiong@email.unc.edu.
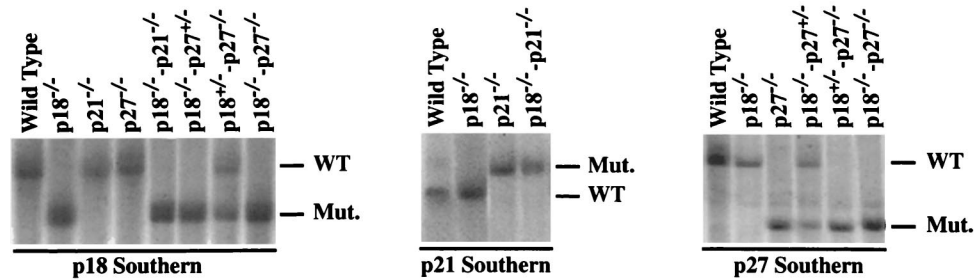† Present address: Department of Biological Science, Purdue University, West Lafayette, IN 47907-1392.

FIG. 1. Genotypic analysis of CDK inhibitor genes. Southern blot analysis of p18, p21, and p27 loci. Genomic DNA from the indicated genotypes was digested with *Eco*RV (p18), *Bgl*II (p21), or *Eco*RI (p27) and hybridized with the indicated DNA probes. The wild-type (WT) and targeted null (Mut.) alleles are indicated.

higher tumor incidence when challenged with γ-irradiation (9), and that Rb$^{+/-}$-p27$^{-/-}$ mice developed more aggressive pituitary adenoma and thyroid C-cell carcinomas than the Rb$^{+/-}$ mice (27). The lack of more widely spread tumors in these single-knockout mice may, in part, be due to a redundant or overlapping function for many of these CDK inhibitors in specific tissues. To test the possibility that different CDK inhibitor genes may functionally collaborate to suppress tumor growth with different tissue specificities, we have characterized the tumorigenesis of two strains of double mutant mice lacking either p18 and p27 or p18 and p21.

MATERIALS AND METHODS

Creation of double null mice. Genetic disruptions of the p18 (11), p21 (6), and p27 (19) loci have been previously described. Mice deficient for both p18 and p21 were created by mating p18$^{-/-}$ and p21$^{-/-}$ mice (6). The resulting F$_1$ p18$^{+/-}$-p21$^{+/-}$ mice were crossed to create the double null genotype. The creation of the p18$^{-/-}$-p27$^{-/-}$ strain as well as the intermediate "3/4" mutant strains (p18$^{+/-}$-p27$^{-/-}$ and p18$^{-/-}$-p27$^{+/-}$) have been previously described (11). All of the p18-p21 and p18-p27 genotypes (wild type, p18$^{-/-}$, p21$^{-/-}$, p27$^{-/-}$, p18$^{-/-}$-p21$^{-/-}$, and p18$^{-/-}$-p27$^{-/-}$) are on a mixed C57BL/6-129 genetic background. For each genotype, intercrosses have been carried out to F$_9$ or F$_{10}$ generations without any alteration of the observed phenotypes resulting from genetic background effects. All genotypes were confirmed by Southern blot analysis (6, 11, 19).

Anatomic and histologic analysis. Many animals were sacrificed and subjected to complete necropsy at the first indication of morbidity (weight loss, dehydration, ataxia, or failure to thrive). Other animals (primarily wild-type or single null animals) were sacrificed as age-matched controls. Several animals were sacrificed between 12 and 17 months of age to analyze age-related tumor progression. Body and organ weights were measured for every animal during necropsy. For histological analysis, tissues were fixed and processed as previously described (11). Testes were fixed in Bouins' solution.

Antibodies and immunochemistry. Antisera for p18, p21, p27, CDK2, CDK4, and CDK6 and procedures for immunoprecipitations, immunoblotting, and kinase assays have been previously described (11, 12, 16, 28, 38). Protein lysate concentrations were determined by the Bradford assay and equalized for each experiment. All Western analysis and kinase assays were performed at least twice using independent sets of 3-month-old tissue lysates. Equal loading of lysates was further verified by tubulin (Neomarkers, Freemont, Calif.) Western blot analysis. Procedures for calcitonin (Dako Corporation, Carpinteria, Calif.) immunohistochemistry were carried out according to the manufacturer's suggested protocol. Leydig cells were selectively immunostained with a monoclonal antibody, LC-6H6 (15), which recognizes an antigen on the surface of Leydig cells, or with an antibody against estrogen sulfotransferase (34), a Leydig cell cytosolic enzyme. Immunostaining was visualized using the avidin-biotin-immunoperoxidase method with diaminobenzidine as the substrate (Vectastain ABC; Vector Laboratories, Burlingame, Calif.). Calcitonin and Leydig-specific immunostaining was performed on tissue sections from several animals of all genotypes.

Kinase assays. Kinase assays have been previously described (11). Briefly, cell lysate was prepared in ice-cold NP-40 lysis buffer from different tissues with different genotypes and precipitated with a specific antibody for 2 h at 4°C with rotation. Five micrograms of affinity-purified anti-mouse CDK4 antibody or 1 μl of crude anti-CDK2 serum was used to immunoprecipitate 2 mg of cell lysate. Protein A-agarose beads were added and incubated for 1 h with rotation at 4°C to precipitate immunoglobulin. The beads were washed twice with NP-40 lysis buffer and once in kinase assay buffer. The washed beads were resuspended in 25 μl of kinase assay buffer containing 5 μCi of [γ-^{32}P]ATP and 2 μg of GST-pRb^{C137} substrate (a fusion protein of glutathione-*S*-transferase [GST] and the C-terminal 137 amino acids of pRb) for CDK4 or 4 μg of histone H1 substrate

(Boehringer Mannheim) for CDK2 kinase assays. The reaction mix was incubated at 30°C for 30 min, and the reaction was terminated by adding 20 μl of 2× loading dye (100 mM Tris-HCl [pH 6.8], 4% sodium dodecyl sulfate [SDS], 20% glycerol, 0.2% bromophenol blue, 0.2 M dithiothreitol). Ten microliters of CDK2 or CDK4 reaction samples was resolved by SDS–15% polyacrylamide gel electrophoresis (PAGE). To verify equal loading, the gel was stained with Coomassie blue to visualize immunoglobulin and substrate proteins before it was dried and exposed to X-ray film. Following exposure to X-ray film, the dried gels were exposed to phosphorimaging plates. ^{32}P incorporation was quantitated on a PhosphorImager.

RESULTS

Generation of p18-p27 and p18-p21 double null mice. We previously found that the progression of pituitary tumors was greatly accelerated by the simultaneous loss of both p18 and p27 genes and that double null mice invariably died by 3 months of age (11). To determine whether p18 and p27 may also function in suppressing tumor growth in other tissues, we carried out a more detailed histological analysis in the p18-p27 double null mice (*n* = 33), especially in tissues where loss of either p18 or p27 had previously been shown to cause detectable abnormal growth. To determine the specificity of functional collaboration between different CDK inhibitor genes, we also generated double mutant mice lacking both p18 and p21 genes and examined both the incidence and spectrum of tumor development (*n* = 18). Because the accelerated mortality of p18-p27 double null mice might potentially exclude the detection of later-developing tumors, we also generated mice retaining one allele of either p18 or p27 (p18$^{-/-}$-p27$^{+/-}$ or p18$^{+/-}$-p27$^{-/-}$; hereafter referred to as 3/4 mutant mice). The 3/4 mutant animals have an extended life span (average, 9 months) beyond that of double null mice, thereby allowing examination for later-developing tumor growth. The p18-p21 double null mice can live beyond 14 months without detectable increase in mortality, and thus no 3/4 mutant p18-p21 mice were analyzed.

p18-p27 mutant mice were generated by crossing p18$^{-/-}$ mice with mice disrupted in the cyclin-CDK inhibition domain of p27 (11, 19). Mice lacking p18 and p21 genes were generated by crossing p18$^{-/-}$ mice with mice deleted for p21 exon 2, which removes 90% of the p21 coding sequence (6). Various genotypes were verified by Southern blot analysis (Fig. 1) and PCR (data not shown). One of the characteristic phenotypes of both p18- and p27-deficient mice is the development of gigantism and widespread organomegaly (10, 11, 19, 23). Many of these organs (e.g., adrenal, thyroid, and testis) from p18-p27 double mutant mice displayed an even greater disproportionate organomegaly (data not shown). Like the mating between p18$^{+/-}$ and p27$^{+/-}$ mice (11), mating between p18$^{+/-}$ and p21$^{+/-}$ mice produced all genotypes at the anticipated Mendelian ratios, indicating that embryos with partial or complete loss of p18 and p21 functions are viable (data not shown). Thirty p18$^{-/-}$-p21$^{-/-}$ mice monitored between 5 and 14

TABLE 1. Spontaneous tumor formation and incidence in p18-, p27-, "3/4"- and p18/27-deficient mice[a]

Organ	Wild type (n = 63)	p18$^{-/-}$ (n = 42)	p27$^{-/-}$ (n = 24)	p18$^{-/-}$-p27$^{+/-}$ (n = 25)[b]	p18$^{+/-}$-p27$^{-/-}$ (n = 6)[b]	p18$^{-/-}$-p27$^{-/-}$ (n = 33)[c]
Pituitary						
Normal	58/58	4/37	7/20	1/25	0/5	0/33
Hyperplasia		22/37[d]	8/20[d]	6/25	0/5	2/33
Adenoma		10/37[e]	5/20[e]	18/25	5/5	30/33
Carcinoma		1/37[f]				1/33
Adrenal						
Normal	58/58	14/24	12/21	10/24	1/6	0/23
Medullary hyperplasia		8/24	4/21	10/24	2/6	2/23
Pheochromocytoma		2/24[f]	5/21	4/24	3/6	21/23[g]
Thyroid						
Normal	63/63	36/42	23/24	11/24	3/4	2/16
C-cell hyperplasia		5/42[f]	1/24	11/24	0/4	13/16
C-cell adenoma		1/42[f]		2/24	1/4	1/16
Testis						
Normal interstitium	27/27	1/41	12/12	2/17	4/5	0/10
Interstitial hyperplasia		39/41		9/17	1/5	10/10
Interstitial adenoma		1/41[h]		6/17		
Parathyroid						
Normal	19/19	11/12	11/11	5/8	3/3	6/6
Hyperplasia		0/12		2/8		
Adenoma		1/12[k]		1/8		
Pancreas						
Normal	16/17	15/15	14/14	6/9	3/3	4/5
Islet cell hyperplasia	1/17[i]			3/9		1/5
Stomach						
Normal	63/63	39/39	19/23	20/21	3/6	5/14
Squamous hyperplasia			3/23	1/21	3/6	6/14
Squamous papilloma			1/23			3/14
Neuroendocrine hyperplasia						1/14
Intestine (duodenum)						
Normal	59/59	39/39	19/24	20/23	4/4	2/17
Focal hyperplasia[j]			0/24	3/23		5/17
Villous adenoma[j]			5/24			10/17
Lungs						
Normal	35/35	24/24	19/20	17/18	6/6	24/24
Histiocytic pneumoniae			1/20	1/18		
Bronchioalveolar adenoma						
Bronchioalveolar carcinoma						
Liver, normal	35/35	24/24	21/21	17/17	6/6	24/24

[a] The numbers in the column heads are the total number of animals examined unless stated otherwise. Data are presented as number positive/number examined.
[b] These mice died by 8 to 9 months of age.
[c] These mice died by 3.5 months of age.
[d] Tumors developed on average by 2 to 4 months.
[e] Tumors developed on average by 7 to 11 months.
[f] Mice more than 12 months old.
[g] One tumor metastasized to a pelvic nerve.
[h] Mouse 16 months old.
[i] Mouse >22 months old.
[j] Focal lesions of Brunner's gland.
[k] Mouse 11 months old.

months of age appeared developmentally normal and did not exhibit any apparent enhancement of the p18$^{-/-}$ gigantism and organomegaly phenotypes (data not shown). In distinct contrast to p18$^{-/-}$-p27$^{-/-}$ mice, which invariably died at between 3 and 4 months of age, p18$^{-/-}$-p21$^{-/-}$ mice demonstrated no decreased survival. These results suggest that p18 functionally collaborates with p27 but not with p21 in controlling organ size and body weight.

Different spectra of tumor development in p18-p27 and p18-p21 double null mice. In addition to the previously described pituitary adenoma (11), the p18-p27 mutant mice, including both double null and 3/4 mutant animals, frequently developed hyperplasia, adenomas, and/or carcinomas in seven other tissues: the adrenal, thyroid, and parathyroid glands, testis, stomach, duodenum, and pancreas (Table 1). With the exception of

pituitary adenomas, these tumors were rarely seen in either single null strain. Invariably, p18$^{-/-}$-p27$^{-/-}$ animals died around the age of 3 months and the 3/4 mutant animals died at an average age of about 9 months from massive pituitary neoplasms. These results further confirm the functional redundancy between p18 and p27 genes and revealed a much broader function of these two CDK inhibitor genes in tumor suppression than previously recognized.

Examination of p18-p21 double null mice (n = 18) revealed a different and more confined spectrum of tumor growth (Table 2). Except for one animal, all of the p18-p21 double null mice developed pituitary pathology (hyperplasia or adenomas) by the age of 12 to 13 months (Table 2). At this age, about half of the p18$^{-/-}$ mice showed pituitary hyperplasia and the remainder had pituitary adenomas. Although only a few p21 null

TABLE 2. Spontaneous tumor formation and incidence in p18-, p21-, and p18/21-deficient mice over 1 year[a]

Organ	Wild type ($n = 17$)	p18$^{-/-}$ ($n = 18$)	p21$^{-/-}$ ($n = 22$)	p18$^{-/-}$-p21$^{-/-}$ ($n = 18$)
Pituitary				
Normal	17/17	2/18	18/21	1/17
Hyperplasia		8/18	3/21	1/17
Adenoma		7/18		15/17
Carcinoma		1/18[b]		
Stomach				
Normal	17/17	16/16	17/22	2/18
Neuroendocrine hyperplasia			5/22	16/18
Lungs				
Normal	17/17	15/15	20/21	9/17
Histiocytic pneumoniae			1/21	5/17
Bronchioalveolar adenoma				2/17
Bronchioalveolar carcinoma				1/17[e]
Liver				
Normal	17/17	15/15	22/22	14/16
Hepatic nodular hyperplasia				2/16
Adrenal				
Normal	15/15	7/17	19/19	1/13
Medullary hyperplasia		8/17		12/13
Pheochromocytoma		2/17[c]		
Thyroid				
Normal	17/17	12/18	22/22	15/17
C-cell hyperplasia		5/18		2/17
C-cell adenoma		1/18[d]		
Testis				
Normal interstitium	5/5	5/15	10/10	1/9
Interstitial hyperplasia		14/15		8/9
Interstitial adenoma		1/15		
Parathyroid				
Normal	17/17	15/15	16/16	12/14
Hyperplasia				2/14
Pancreas				
Normal	16/17	15/15	20/20	11/12
Islet cell hyperplasia	1/17			1/12
Intestine (duodenum), normal	17/17	15/15	18/18	15/15

[a] See Table 1, footnote a.
[b] Invasion of neurohypophysis by intermediate-lobe tumor cells.
[c] Bilateral.
[d] One metastatic tumor composed of poorly demarcated nonencapsulated hypercellular foci with collapsed follicles separated by dense interstitial infiltrates of lymphocytes.
[e] Tumor implants in alveoli distant from original tumor.

mice developed slight pituitary hyperplasia, loss of p21 function accelerated the incidence and progression of pituitary pathology initiated by the loss of p18. It should be noted that the loss of p18 and p21, like the loss of p18 and p27, enhanced the pituitary tumor phenotype in this tissue. Therefore, in this case, the accelerated pituitary tumor growth represents a functional collaboration between p18 and p21 rather than distinct tissue specificity from that of p18 and p27. Tissue specificity of tumor suppression is more apparent when comparing the p18-p27 double mutant mice with p18-p21 double mutant mice in other tissues, where clear tissue differences are observed (e.g., thyroid or duodenum in p18-p27 mice and lung in p18-p21 mice).

Nearly all p18-p21 double null mice developed multifocal gastric neuroendocrine cell hyperplasia. Gastric neuroendocrine cell hyperplasia was detected in a few p21$^{-/-}$ mice and

was not found in any p18$^{-/-}$ mice. At a lower incidence, p18-p21 double null mice developed lung bronchioalveolar adenoma or carcinoma. Two p18-p21 double null mice also exhibited hepatic nodular hyperplasia. These results provide the first genetic evidence for a tumor suppression function of p21. In six tissues where p18-p27 double mutant mice developed frequent hyperplasia or tumors (adrenal, thyroid, testis, parathyroid, pancreas, and duodenum), there is no evidence that p18-p21 losses of function collaborate in tumor development (Table 2). Conversely, p18 and p27 do not seem to collaborate significantly in the formation of gastric neuroendocrine cell hyperplasia, lung tumors, or liver hyperplasia. The distinct tumor spectra of p18-p27 and p18-p21 double null mice indicate that functional collaboration between different CDK inhibitors suppresses tumor growth with different tissue specificities.

p18-p27 double mutant mice develop multiple types of endocrine tumors. Notably, five of the seven tumors that occur in p18-p27 double mutant mice (pituitary adenoma, adrenal pheochromocytoma, thyroid C-cell adenoma, parathyroid adenoma, and testis Leydig cell adenoma), as well as the pancreatic islet cell hyperplasia, all involve endocrine tissues (Table 1 and Fig. 2). This affected tissue spectrum overlaps that seen in patients with type I (MEN1, pituitary, pancreatic, and parathyroid tumors) or type II (MEN2, thyroid C-cell carcinomas, pheochromocytomas, and parathyroid tumors) MEN syndromes. One characteristic feature of MEN syndromes is the concurrent development of multiple endocrine tumors in the same patient. All of the p18$^{-/-}$-p27$^{-/-}$ and most of the 3/4 mutant animals developed multiple endocrine tumors. Most double null animals possessed three or four tumors and had additional hyperplastic tissues. In one p18$^{-/-}$-p27$^{-/-}$ animal, five simultaneous tumors were detected. The most frequently occurring hyperplastic tissues and/or tumors in p18$^{-/-}$-p27$^{-/-}$ mice were the pituitary adenoma and carcinoma (31 of 33, 94%), adrenal medullary hyperplasia and pheochromocytoma (23 of 23, 100%), thyroid C-cell hyperplasia and adenoma (14 of 16, 88%), and testis interstitial cell hyperplasia (10 of 10 males, 100%), all four developing with near or complete penetrance (Table 1). Endocrine lesions found at a lower incidence were parathyroid hyperplasia and adenomas (3 of 8, 38%, p18$^{-/-}$-p27$^{+/-}$ only) and pancreatic islet cell hyperplasia (3 of 9 [33%] in p18$^{-/-}$-p27$^{+/-}$ and 1 of 5 [20%] in double null mice). While the p18-p27 mouse tumors may not exactly mimic those seen in MEN patients (e.g., adenomas in mice instead of carcinomas in humans), the affected cell types (e.g., thyroid C cells, adrenal medullary cells, or pancreatic islet cells) and the spectrum of simultaneous multiple endocrine tissues are strikingly similar. It remains to be determined whether the development of mouse endocrine tumors and human MEN syndrome have a similar molecular mechanism.

By gross examination, adrenal glands of p18$^{-/-}$-p27$^{-/-}$ animals were enlarged compared with age-matched single null or wild-type animals (data not shown). All p18$^{-/-}$-p27$^{-/-}$ mice developed adrenal pathology ($n = 23$, Table 1). Two 3-month-old p18$^{-/-}$-p27$^{-/-}$ mice exhibited severe medullary hyperplasia, while adrenals from the remaining 23 p18$^{-/-}$-p27$^{-/-}$ mice

FIG. 2. p18-p27 double mutant mice developed multiple endocrine tumors. (A) Malignant pheochromocytoma in p18$^{-/-}$-p27$^{-/-}$ adrenal glands. Adrenal cross sections of 3-month-old mice were stained with hematoxylin and eosin. (B) Thyroid C-cell phenotype. The thyroid glands were immunostained for calcitonin. C-cell hyperplasia (CH) in p18$^{-/-}$-p27$^{-/-}$ and C-cell adenomas (A) in p18$^{-/-}$-p27$^{+/-}$ mice are shown. (C) Parathyroid phenotypes. Hematoxylin and eosin staining of parathyroid hyperplasia (PH) and adenoma (PA) in a 7-month-old p18$^{-/-}$-p27$^{+/-}$ mouse. (D) Pancreas phenotype. Hematoxylin and eosin staining of pancreatic islet cell hyperplasia in a 9-month-old p18$^{-/-}$-p27$^{+/-}$ mouse. Several normal (N) and three hyperplastic (ICH) islets are indicated. (E) Testis interstitial cell phenotype. (Left) Interstitial cell adenoma in the testis of a 9-month-old p18$^{-/-}$-p27$^{+/-}$ mouse stained with hematoxylin and eosin. (Right) Interstitial cell hyperplasia in the testis of a 9-month-old p18$^{-/-}$-p27$^{+/-}$ mouse immunostained with monoclonal antibody LC-6H6, which recognizes a Leydig cell constituent.
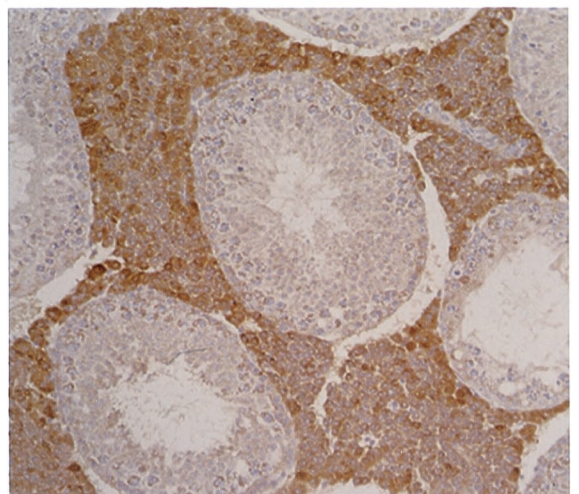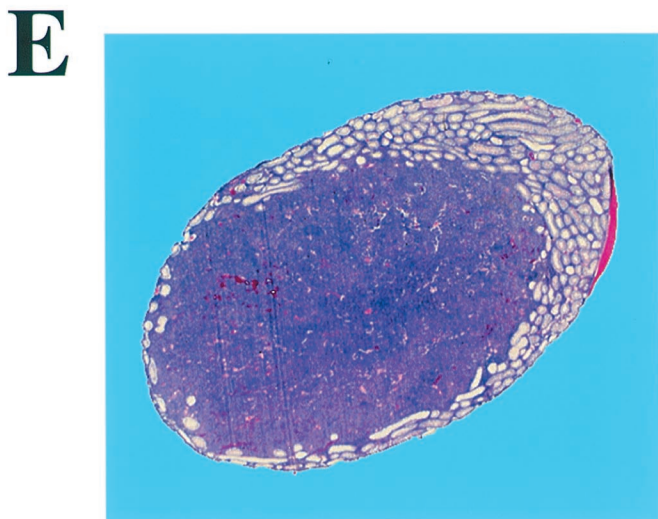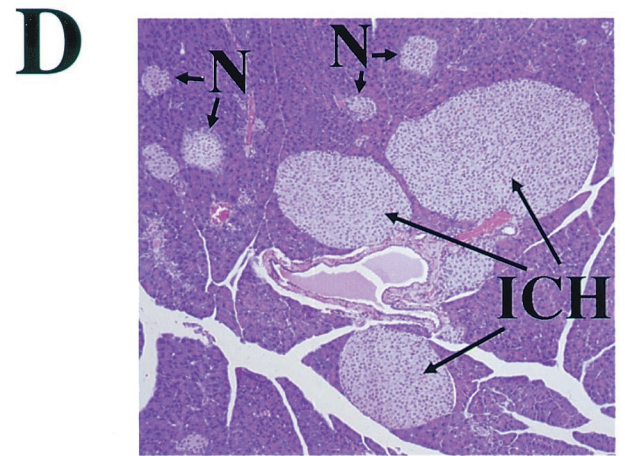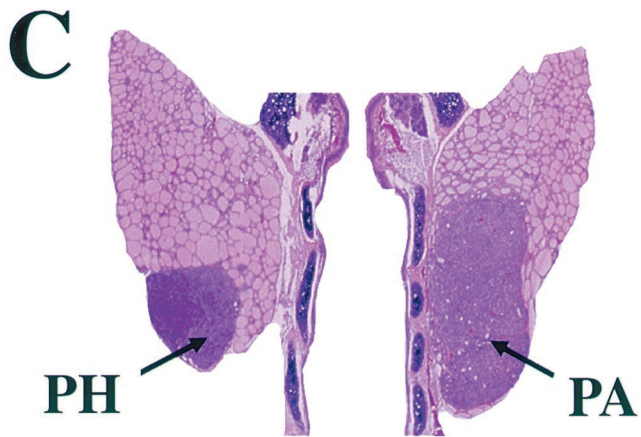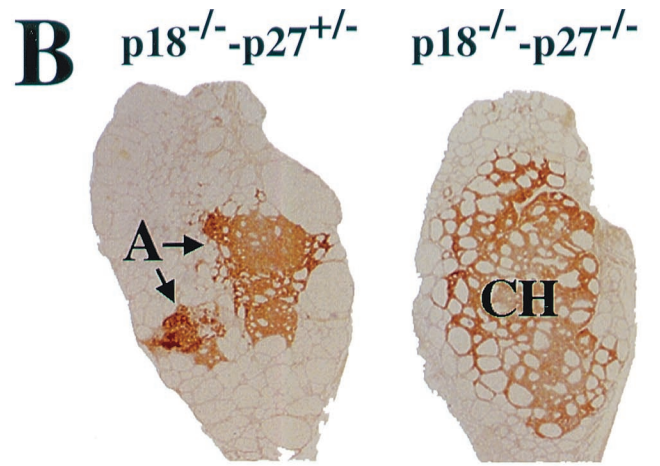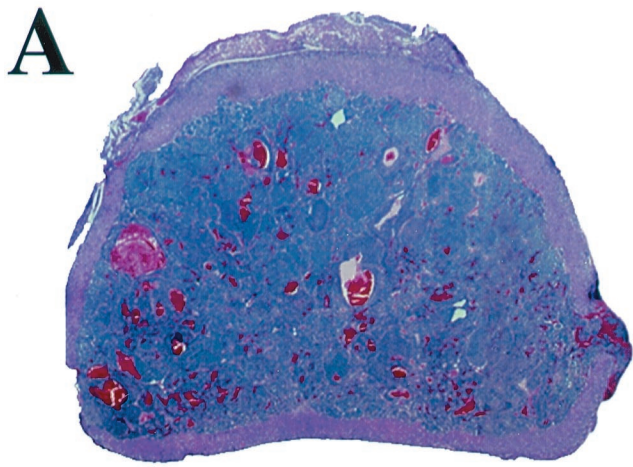
contained bilateral pheochromocytomas (91%) (Fig. 2A). These tumors were detected as early as 1 month and invaded the adrenal cortex in some animals and, in one instance, metastasized to a distal pelvic nerve (data not shown). No adrenal pathology was detected in age-matched 3-month-old wild-type ($n = 7$), $p18^{-/-}$ ($n = 8$), or $p27^{-/-}$ ($n = 9$) animals (data not shown). Although adrenal pathology was detected in some $p18^{-/-}$ or $p27^{-/-}$ animals, the age of detection was never less than 6 months for $p27^{-/-}$ mice or 12 months for $p18^{-/-}$ mice. The earlier age of onset and greater incidence of adrenal phenotypes in p18-p27 double mutants clearly demonstrate that p18 and p27 functionally collaborate in adrenal tumorigenesis.

The thyroid glands of $p18^{-/-}$-$p27^{-/-}$ animals appeared enlarged compared with age-matched single null or wild-type animals (data not shown). Thyroids from most of the 3-month-old $p18^{-/-}$-$p27^{-/-}$ animals revealed C-cell hyperplasia (13 of 16, 81%) (Fig. 2B, right). In addition, three 3/4 mutant mice (3 of 28, 11%) and one $p18^{-/-}$-$p27^{-/-}$ mouse (1 of 16, 6%) developed thyroid C-cell adenomas (Fig. 2B, left). The C-cell origin of these lesions was verified by immunohistochemistry using an antibody to calcitonin, a hormone produced in thyroid C cells (Fig. 2B). Thyroid follicular hyperplasia was occasionally seen in $p18^{-/-}$-$p27^{+/-}$ mice (data not shown). Thyroid glands of seven age-matched 3-month-old wild-type, eight $p18^{-/-}$, and nine $p27^{-/-}$ animals were histologically normal (data not shown). The $p18^{-/-}$ and $p27^{-/-}$ mice that developed thyroid pathology were all over 12 months ($p18^{-/-}$) or 6 months ($p27^{-/-}$) of age.

Parathyroid hyperplasia and/or adenomas were detected in 38% (3 of 8) of the $p18^{-/-}$-$p27^{+/-}$ mice, a lower incidence than seen in the other endocrine tissues (Table 1, Fig. 2C). The average age at detection was 6.8 months. The absence of this phenotype in $p18^{-/-}$-$p27^{-/-}$ mice (0 of 6) may reflect the premature mortality (3 months) of this genotype, while the longer-living $p18^{-/-}$-$p27^{+/-}$ mice (approximately 9 months) survive long enough to develop this phenotype. In addition, 33% of the $p18^{-/-}$-$p27^{+/-}$ (3 of 9) and 20% of the $p18^{-/-}$-$p27^{-/-}$ (1 of 5) mice displayed pancreatic islet cell hyperplasia (Fig. 2D). The age at onset of islet cell hyperplasia was 8.9 months for $p18^{-/-}$-$p27^{+/-}$ mice and 2.9 months for $p18^{-/-}$-$p27^{-/-}$ mice. The lower incidence of islet cell hyperplasia in $p18^{-/-}$-$p27^{-/-}$ mice again may reflect premature mortality and the time required to develop pancreatic islet cell hyperplasia. With the exception of one 22-month-old wild-type mouse, the pancreatic phenotype was not detected in any wild-type (16 of 17), $p18^{-/-}$ (0 of 15), $p27^{-/-}$ (0 of 14), or $p18^{+/-}$-$p27^{-/-}$ (0 of 3) mice. While one wild-type and one $p18^{-/-}$-$p27^{-/-}$ each developed pancreatic islet cell hyperplasia, the increased rate of incidence (6% versus 20%, respectively) and the early age at onset (22 months versus 3 months, respectively) in the double mutant genotype clearly validate the double null result.

In addition to the endocrine tumors commonly seen in MEN patients, the p18-p27 double mutant mice also developed hyperplasia and tumor phenotypes in another endocrine organ, the testis. Gross examination of p18-p27 double null males revealed a marked increase in testicular size by 3 months of age. While $p18^{-/-}$ and $p27^{-/-}$ males also have enlarged testes (10, 11, 23), this phenotype was more pronounced in $p18^{-/-}$-$p27^{-/-}$ males. Mean testis weights of mice (± standard deviation) between 1.5 and 3 months of age varied with genotype, from $0.106 ± 0.004$ mg in wild-type to $0.134 ± 0.009$ mg in $p18^{-/-}$, $0.139 ± 0.023$ mg in $p27^{-/-}$, and $0.206 ± 0.020$ mg in $p18^{-/-}$-$p27^{-/-}$ mice. Testes from $p18^{-/-}$ males (40 of 41, 98%) displayed interstitial cell hyperplasia and/or adenoma

not seen in wild-type ($n = 27$) or $p27^{-/-}$ ($n = 12$) males (Table 1). All p18-p27 double null mice (10 of 10) and all but two of the $p18^{-/-}$-$p27^{+/-}$ males (15 of 17, 88%) also developed interstitial cell hyperplasia. The severity of interstitial cell hyperplasia was always greater in $p18^{-/-}$-$p27^{-/-}$ and $p18^{-/-}$-$p27^{+/-}$ mice than in age-matched $p18^{-/-}$ mice (data not shown). The hyperplastic interstitial cells immunostained with antibodies that recognize Leydig cell constituents (Fig. 2E, right), including monoclonal antibody LC-6H6 (15) and an antibody to estrogen sulfotransferase (34). Compared with $p18^{-/-}$ males, the immunostaining intensity in $p18^{-/-}$-$p27^{-/-}$ and $p18^{-/-}$-$p27^{+/-}$ mice was reduced in regions where interstitial cells were densely packed with little cytoplasm, morphological changes consistent with impaired pituitary function (2). Adenomas were detected in the interstitial cell compartment in six of the $p18^{-/-}$-$p27^{+/-}$ males between 6 and 9 months of age (6 of 17, 35%). This tumor was detected in only one $p18^{-/-}$ male that was 16 months old (1 of 41, 2%). One $p18^{-/-}$-$p27^{+/-}$ male had an adenoma that filled ~80% of the volume of one testis (Fig. 2E, left), with a smaller adenoma present in the other testis. Again, the absence of interstitial cell adenomas in p18-p27 double null mice may result from their early mortality. Clearly, even the absence of one p27 allele is sufficient to accelerate the Leydig cell pathology that results from the loss of p18 function.

Gastrointestinal tumors and hyperplasia in p18-p27 mice. $p18^{-/-}$-$p27^{-/-}$ mutant mice developed two additional nonendocrine lesions: squamous cell hyperplasia and papillomas in the forestomach, and duodenal hyperplasia and villous adenomas (Table 1 and Fig. 3). The squamous cell lesions were focal and always located near the esophageal inlet. The mouse forestomach is normally lined with squamous mucosa, and the hyperplasia observed in $p18^{-/-}$-$p27^{-/-}$ and 3/4 null animals is not a metaplastic occurrence. The duodenal lesions only appeared just distal to the pylorus in conjunction with proliferation of the Brunner's glands. Incidences of the gastrointestinal lesions in $p18^{-/-}$-$p27^{-/-}$ animals were 43% (6 of 14) for squamous cell hyperplasia, 21% (3 of 14) for forestomach papillomas, 29% (5 of 17) for duodenal hyperplasia, and 59% (10 of 17) for duodenal villous adenomas. Neither tumors nor hyperplasia were detected in these tissues in any wild-type ($n = 59$) or $p18^{-/-}$ ($n = 39$) animals. The incidence of these phenotypes in $p27^{-/-}$ ($n = 24$) animals was significantly less than in the $p18^{-/-}$-$p27^{-/-}$ mice.

p18-p21 double null mice develop pathology distinct from p18-p27 mice. The p18-p21 double null mice developed different spectra of tumors and hyperplastic tissues than p18-p27-deficient mice. The incidence and progression of pituitary adenoma were both greatly increased in p18-p21 double null mice compared with $p18^{-/-}$ mice. By 1 year of age, 44% of $p18^{-/-}$ mice developed pituitary hyperplasia and 44% exhibited adenomas or carcinomas (Table 2). However, by this same age, all but one of the p18-p21 double null mice developed either pituitary hyperplasia (1 of 17, 6%) or adenomas (15 of 17, 88%), with almost all animals now developing pituitary adenomas. Therefore, in a $p18^{-/-}$ background, loss of p21 function greatly enhanced the incidence of pituitary pathology as well as the progression from hyperplasia to adenoma. As in p18- or p27-deficient mice, the pituitary adenomas that developed in the p18-p21 mice originated from the intermediate lobe (as determined by histological examination; data not shown). It should be noted that pituitary tumors from 1-year-old $p18^{-/-}$ or $p18^{-/-}$-$p21^{-/-}$ mice were histologically indistinguishable and these mice did not seem to possess different mortality rates (data not shown). This is in contrast to the short 3-month life span of p18-p27 double null mice.
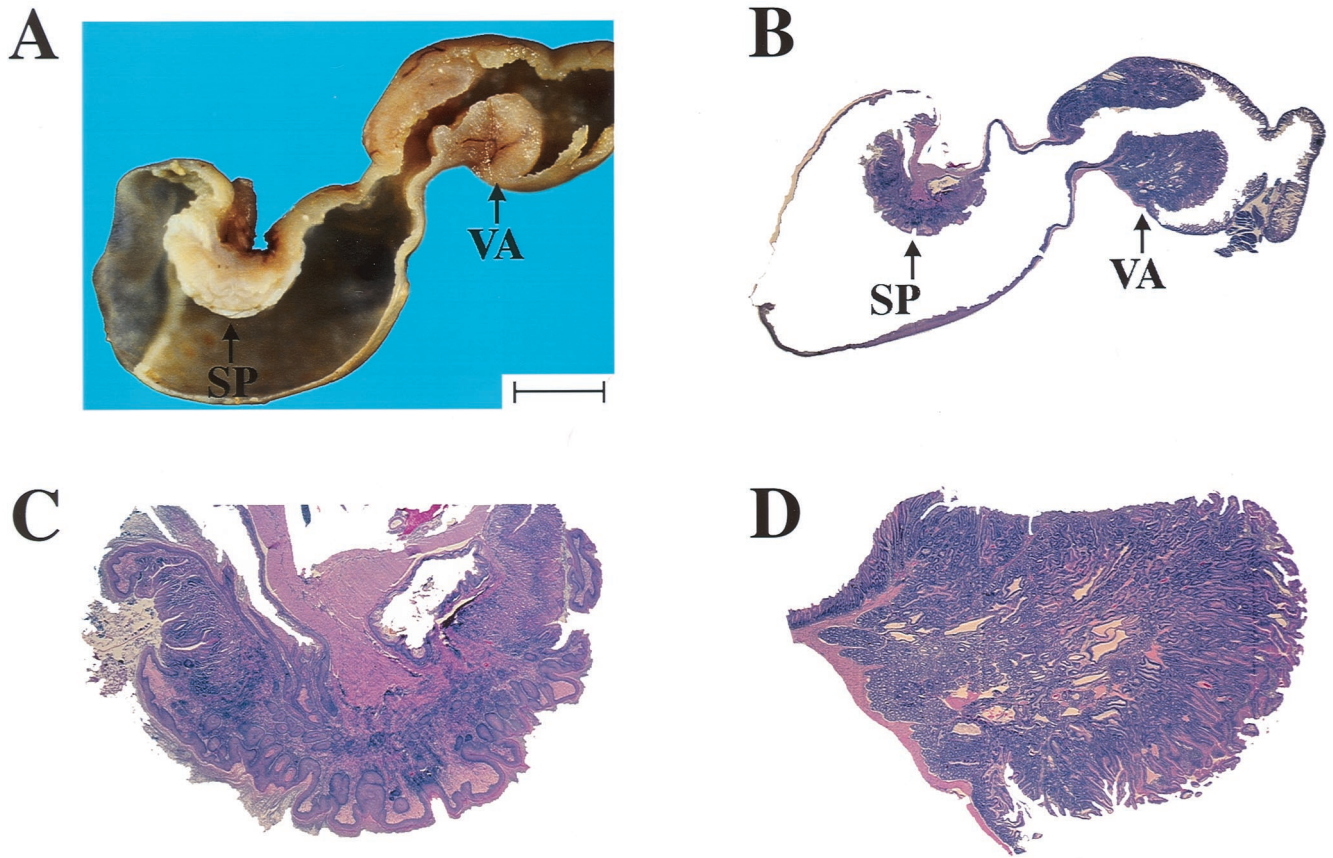
FIG. 3. Nonendocrine tumors in p18-p27 double mutant mice. (A) Gross appearance of stomach squamous cell papillomas (SP) and duodenal villous adenomas (VA) in 3-month-old p18$^{-/-}$-p27$^{-/-}$ mouse. Bar, 5 mm. (B) Hematoxylin and eosin staining of stomach squamous cell papillomas (SP) and duodenal villous adenomas (VA) in 3-month-old p18$^{-/-}$-p27$^{-/-}$ mouse. (C) Stomach squamous cell papilloma from panel B. (D) Duodenal villous adenoma from panel B.

Of 18 p18-p21 double null mice, 89% developed multifocal gastric neuroendocrine cell hyperplasia (Fig. 4A). In one instance, nodules of neuroendocrine cells extended superficially into the subjacent muscular layers of the stomach (Fig. 4B). This could be evidence of local invasion or merely hyperplasia of neuroendocrine cells in a naturally occurring mucosal diverticulum. While local invasion is one of the few histologic indications of malignancy for neuroendocrine cell tumors (carcinoids), the small size and multifocal nature of the lesion in this mouse are more consistent with hyperplasia than carcinoid tumor. Two of 17 p18-p21 mice had bronchioalveolar adenoma (data not shown), and 1 of 17 had a bronchioalveolar carcinoma (Fig. 4C). The presence of lung tumors in 3 of 17 p18-p21 double null mice (18%) combined with the lack of detectable tumors in the lungs of any wild-type or single null animals suggests that these tumors result from loss of p18-p21 functions rather than from normal aging processes. Two p18-p21 double null mice developed hepatic nodular hyperplasia (2 of 16; data not shown), a finding that is not uncommon in older mice of this genetic background (C57BL/6). We therefore cannot dismiss the possibility that this may be an incidental aging lesion and not entirely due to the p18-p21 mutations. Except for pituitary adenomas in p18$^{-/-}$ mice, the tumor phenotypes seen in p18-p21 double null mice were rarely detected in wild-type or either single p18- or p21-null mice. In the six tissues where p18-p27 double mutant mice developed hyperplasia and/or tumors (adrenal, thyroid, testis, parathyroid, pancreas, and duodenum), there is no evidence that p18-p21 loss of

function collaborates in tumor development (Table 2). Also, there is no indication that p18 and p27 significantly collaborate in the formation of gastric neuroendocrine cell hyperplasia, lung tumors, or liver pathology. The distinct spectra of tumors that form in p18-p27 or p18-p21 double mice indicate that functional collaboration between different CDK inhibitors suppresses tumor growth with different tissue specificities.

Gene dosage-dependent tumor suppression in p18-p27 mice. Comparison of mice with five different genotypes—the p18$^{-/-}$ and p27$^{-/-}$ single nulls, the two 3/4 mutants, and the p18$^{-/-}$-p27$^{-/-}$ double null—revealed evidence for gene dosage-dependent tumor suppression by p18 and p27. In many tissues, both 3/4 mutant genotypes exhibited an intermediate phenotype of tumor growth, more aggressive than in either single null animal and in most cases less severe than in the double null mice. This was manifested in both the incidence of tumor formation and the rate of tumor growth. First, the incidence of tumor formation in many tissues of 3/4 null animals was decreased compared to double null mice but was higher compared to either single null mouse strain (Table 1). For example, pheochromocytomas occurred in 95% of p18$^{-/-}$-p27$^{-/-}$ mice but only in 16% of the p18$^{-/-}$-p27$^{+/-}$ mice and 60% of the p18$^{+/-}$-p27$^{-/-}$ mice despite the longer life span of 3/4 mutant animals. Forestomach hyperplasia and adenomas were detected in 62% of the double null mice, with hyperplasia detected in only 5% of the p18$^{-/-}$-p27$^{+/-}$ mice and 40% of the p18$^{+/-}$-p27$^{-/-}$ mice. Duodenal hyperplasia and adenomas were detected in 88% of the double null mice, with hyperplasia
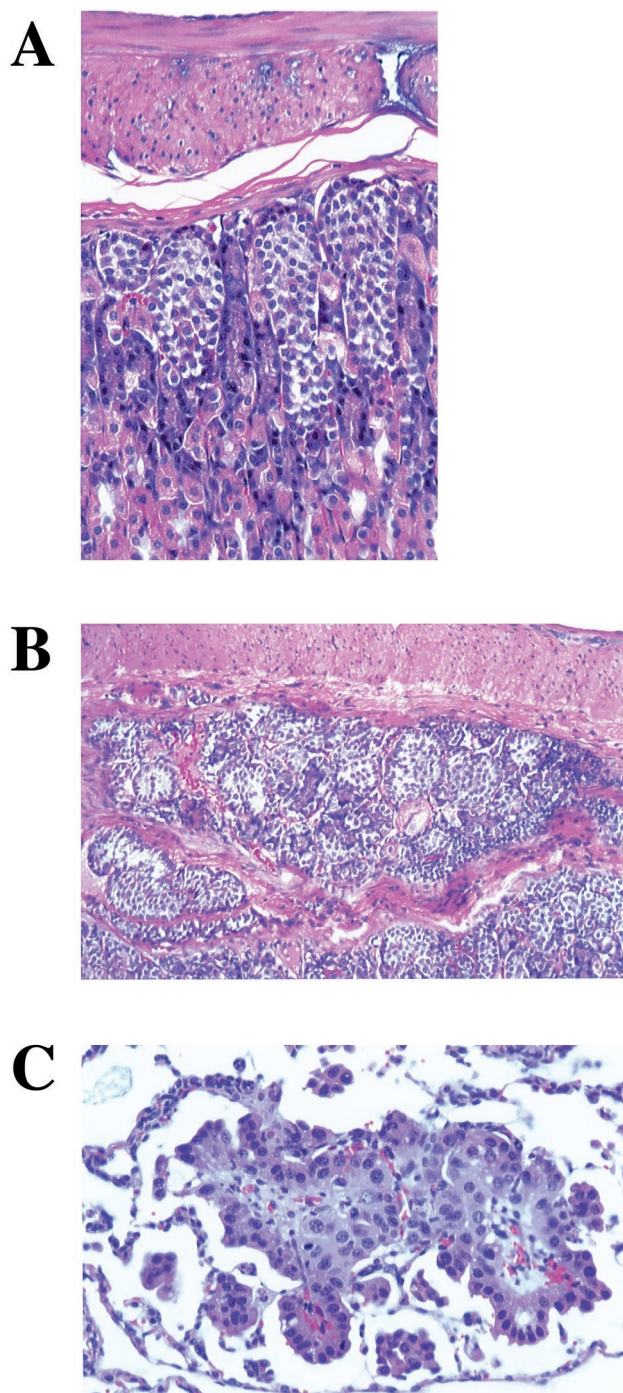
FIG. 4. Tumor phenotypes in p18-p21 double null mice. (A) Hematoxylin and eosin staining of multifocal gastric neuroendocrine cell hyperplasia in 12-month-old $p18^{-/-}$-$p21^{-/-}$ mouse. (B) Hematoxylin and eosin staining of gastric neuroendocrine cell hyperplasia in a 12-month-old $p18^{-/-}$-$p21^{-/-}$ mouse showing extension of neuroendocrine cells into the muscular layer of the stomach. (C) Hematoxylin and eosin staining of lung bronchioalveolar carcinoma in 12-month-old $p18^{-/-}$-$p21^{-/-}$ mouse.

only detected in 13% of the $p18^{-/-}$-$p27^{+/-}$ mice. Gastrointestinal tumors were not seen in 3/4 mutant animals (Table 1). Other than pituitary adenomas and with the previously noted infrequent exceptions, tumors either did not develop or were rarely seen in wild-type or either single null genotypes (Table

1). In some tissues, the 3/4 null mice developed tumors that were not detected in the double null mice. As previously mentioned, we interpret this as a result of the early mortality of the double null animals. Because the 3/4 null mice live longer (9 months) than the double null mice (3 months), perhaps they have sufficient time for further initiation and/or progression of tumor formation. Second, the rate of tumor growth in some tissues was slower in 3/4 mutant animals than in $p18^{-/-}$-$p27^{-/-}$ mice, but was accelerated compared with either single null mouse strain. The average age at pituitary tumor formation was 2.7 months in $p18^{-/-}$-$p27^{-/-}$ mice and 7.4 months in 3/4 mutant mice. Accordingly, the average life span increased from 3 months in the double null mice to an average of 9 months in both types of 3/4 mice. In comparison, $p18^{-/-}$ mice (9 of 31) developed pituitary tumors at an average age of 11 months, while $p27^{-/-}$ mice (4 of 16) developed this tumor at an average age of 7.6 months, and both single null genotypes routinely live well beyond 1 year. Similarly, the pheochromocytoma developed by 2.6 months in $p18^{-/-}$-$p27^{-/-}$ mice and 7.3 months in 3/4 mutant mice.

Conceivably, enhancement of neoplastic transformation in 3/4 animals compared with single null mice could be caused by an increased incidence of loss of heterozygosity that removes the remaining wild-type allele. Three lines of evidence argue against this possibility. First, mice heterozygous for p27 display intermediate phenotypes in both body size and organ weights without the loss of heterozygosity (10, 19, 23). Second, both the p18 and p27 genes appear to be quite stable in the genome and are rarely mutated or deleted. Third, intermediate phenotypes were seen in both types of 3/4 genotypes and in many different organs (Table 1). Consistent with the notion that functional loss of the remaining wild-type allele is not the primary cause for the augmented phenotypes seen in the 3/4 mice, we have found no evidence for the loss of the remaining p27 allele in multiple samples from three different types of tumors (pituitary, adrenal, and thyroid) derived from $p18^{-/-}$-$p27^{+/-}$ mice by Southern blot analysis (data not shown).

Tissue expression of CDK inhibitors. To confirm that p18, p21, and p27 are normally expressed in the organs where pathology developed in the mutant mice, we examined various wild-type tissues by Western blot analysis for expression of p18, p21, and p27 proteins as well as their two common targets, CDK4 and CDK6 (Fig. 5). CDK4 and CDK6 were expressed in all of the tissues examined. Expression of p18 was highest in the intestines, kidney, liver, pituitary, skeletal muscle, stomach, testes, and thyroid, although expression was detectable in all of the tissues examined. p21 was expressed in the adrenal, intestines, lung, pituitary, spleen, stomach, testes, thymus, and thyroid, with low expression detected in the heart and liver. p27 was expressed in all of the tissues examined, with highest expression in the adrenal gland, heart, pituitary, and skeletal muscle. Importantly, expression of the CDK inhibitors was consistent with the tissues where p18, p21, or p27 loss of function caused the development of hyperplastic or tumorigenic phenotypes. For example, p18-p21 double null mice develop pituitary, gastric neuroendocrine cell, and lung tumors. Both proteins are expressed in the pituitary, stomach, and lung. Mice lacking both p18 and p27 exhibit tumor growth in the adrenal, intestines, pituitary, stomach, testes, and thyroid (including parathyroid), all tissues where p18 and p27 are readily detectable. It should be pointed out that in some tissues, the expression of these genes is clearly detected (e.g., p21 in adrenal and p27 in lung), yet loss of CDK inhibitor function does not result in obvious tumor phenotypes. This suggests that p18, p21, or p27 is not a rate-limiting factor for tumor formation in any tissue where it is expressed.
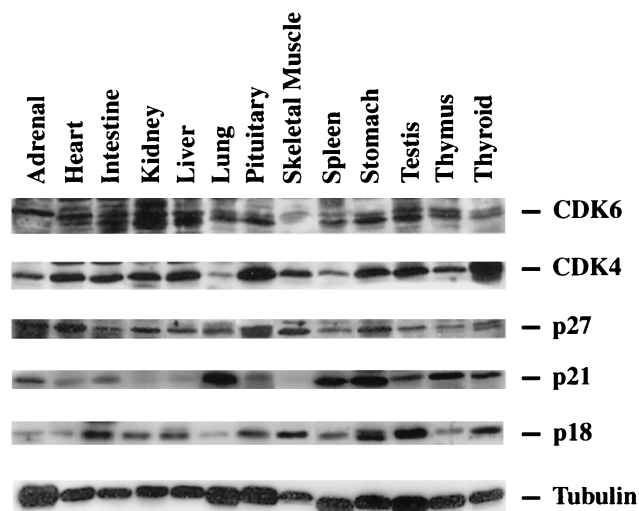
FIG. 5. Expression of CDK and CDK inhibitors in mouse tissues. Total cell lysates were prepared from the indicated wild-type tissues. Expression patterns of CDK4, CDK6, p27, p21, p18, and tubulin were determined by Western blot analysis. Tubulin expression was used to demonstrate equal loading of protein lysates.

Simultaneous loss of p18 and p27 increases G_1 CDK kinase activity. To provide a plausible molecular mechanism for the development of the tumorigenic phenotype in these CDK inhibitor-deficient mice, we compared the kinase activity of two G_1 CDKs, CDK2 and CDK4, in mice of various genotypes using either histone H1 (for CDK2) or GST-pRb (for CDK4) as substrates. We chose four tissues, adrenal gland, testis, lung, and skeletal muscle, from 3-month-old animals for this analysis. At this age, hyperplastic or tumor phenotypes were consistently detected in p18$^{-/-}$-p27$^{-/-}$ adrenal gland and testis, but not in lung and skeletal muscle tissue or in mice of several other genotypes (Tables 1 and 2). Such analysis would potentially allow us to determine whether any change in kinase activity precedes or follows cell transformation.

Compared with wild-type adrenal tissue, H1 kinase activity of CDK2 remained essentially unchanged in p21$^{-/-}$ and p18$^{-/-}$ lysate, increased about 2.4-fold in p27$^{-/-}$ lysate (varying between 1.5- and 3-fold in different experiments), 1.7-fold in p18$^{-/-}$-p21$^{-/-}$ lysate, and 6-fold in p18$^{-/-}$-p27$^{-/-}$ lysate (Fig. 6A). Rb kinase activity of CDK4 increased in all five mutant adrenal tissues: 2-fold in p18$^{-/-}$ lysate, 4-fold in p21$^{-/-}$ lysate, 6-fold in p18$^{-/-}$-p21$^{-/-}$ lysate, 6-fold in p27$^{-/-}$ lysate, and 12-fold in p18$^{-/-}$-p27$^{-/-}$ lysate. The testis CDK2 kinase activity increased two- to fourfold in p18$^{-/-}$ lysate, four- to sixfold in p27$^{-/-}$ lysate, and synergistically increased about eightfold in p18$^{-/-}$-p27$^{-/-}$ testis lysate (Fig. 6B). Loss of p21 had little effect on testis CDK2 kinase activity as seen in either p21$^{-/-}$ or p21$^{-/-}$-p18$^{-/-}$ lysate. The testis Rb kinase activity of CDK4 increased two- to threefold in p18$^{-/-}$ lysates, twofold in p21$^{-/-}$ lysates, four- to sixfold in p27$^{-/-}$ lysates, fourfold in p18$^{-/-}$-p21$^{-/-}$ lysates, and six- to sevenfold in p18$^{-/-}$-p27$^{-/-}$ lysates. These results suggest that associated with the development of hyperplastic growth in both the adrenal gland and testis, the activity of both CDK2 and CDK4 kinase was increased by the loss of p18 or p27, and the simultaneous loss of both genes synergistically stimulated the activity of both CDKs.

To determine whether the increase in CDK activity is consequent to the development of tumor pathology, we determined both CDK2 and CDK4 kinase activity in two additional tissues, the lung and skeletal muscle, that possessed no observable tumor phenotypes at 3 months of age. The lung CDK2 activity was increased approximately twofold in p21$^{-/-}$, p27$^{-/-}$, p18$^{-/-}$-p21$^{-/-}$, and p18$^{-/-}$-p27$^{-/-}$ genotypes with no apparent synergistic effects. Lung CDK4 activity was unchanged in p18$^{-/-}$ or p21$^{-/-}$ lysates and was increased approximately threefold in p27$^{-/-}$, p18$^{-/-}$-p21$^{-/-}$ and p18$^{-/-}$-p27$^{-/-}$ genotypes. In the skeletal muscle, CDK2 activity was increased approximately twofold in p18$^{-/-}$ and p21$^{-/-}$ lysates and approximately four to sixfold in p27$^{-/-}$, p18$^{-/-}$-p21$^{-/-}$, and p18$^{-/-}$-p27$^{-/-}$ lysates. The Rb kinase activity of CDK4 was increased approximately 2-fold in p18$^{-/-}$ or p21$^{-/-}$ lysates, 7- to 8-fold in p27$^{-/-}$ or p18$^{-/-}$-p21$^{-/-}$ lysates, and 12-fold in p18$^{-/-}$-p27$^{-/-}$ lysate.

These results provide a plausible biochemical basis—increase in G_1 CDK2 and CDK4 kinase activity—for the hyperplastic and tumor growth observed in the absence of p18, p21, and p27. Increase in CDK2 and CDK4 kinase activity is not dependent on and most likely precedes the development of tumor phenotypes. While an altered proportion of cell types resulting from hyperplastic growth and/or tumorigenesis could potentially contribute to the change in kinase activity in double null tissues, this would not explain the increase in kinase activity in single null tissues where the hyperplastic phenotypes were not as pronounced or were absent (e.g., skeletal muscle and lung). We therefore interpret the increased kinase activity in the single and double null tissues to be a direct effect of the disruption of p18, p21, and/or p27. In many cases, simultaneous loss of two CDK inhibitor genes synergistically increased CDK activity. This is consistent with accelerated tumorigenesis in double mutant mice and suggests that the level of CDK kinase activity is a rate-limiting factor for the tumor growth. These results also indicate that an increase in G_1 CDK activity alone is not sufficient to initiate tumor growth in some tissues (e.g., lung and skeletal muscle) and additional genetic changes are required. Finally, an increase in CDK4 kinase activity in all four p21- and p27-deficient tissues, adrenal, skeletal, lung, and testis, was somewhat unexpected, given the recent report that loss of either p21 or p27 impaired the assembly of cyclin D-CDK4 complex and decreased Rb kinase activity of CDK4 in in vitro-cultured mouse embryo fibroblasts (5). This finding raises the possibility that assertion of the role of p21 and p27 as positive regulators of CDK4 may be dependent on cell types or in vivo and in vitro kinase assay conditions.

DISCUSSION

In this report, we provided the first evidence that functional collaborations between different CDK inhibitor genes suppress tumor growth with distinct tissue specificities. Previously, collaboration between different CDK inhibitors has been thought to contribute to differentiation of eye lens fiber cells (42) and muscle (43), but not in general tissue tumor suppression. Our results indicate that p18, p21, and p27 can indeed function together as tumor suppressor genes. We have found that, except for the pituitary, there is no overlap in the tumor spectrum between p18$^{-/-}$-p27$^{-/-}$ and p18$^{-/-}$-p21$^{-/-}$ mice. While the loss of both p18 and p27 resulted in spontaneous development of multiple tumors, predominantly in endocrine organs, p18-p21 double null mice developed pituitary adenomas, gastric neuroendocrine cell hyperplasia, and lung bronchioalveolar tumors. Therefore, with the exception of pituitary tumors, the cooperative tumor suppressor activities of p18-p21 and p18-p27 function with tissue specificity. p21 functions as the major downstream target of p53 to cause G_1 cell cycle arrest in response to DNA damage (3, 6, 8), predicting a tumor sup-
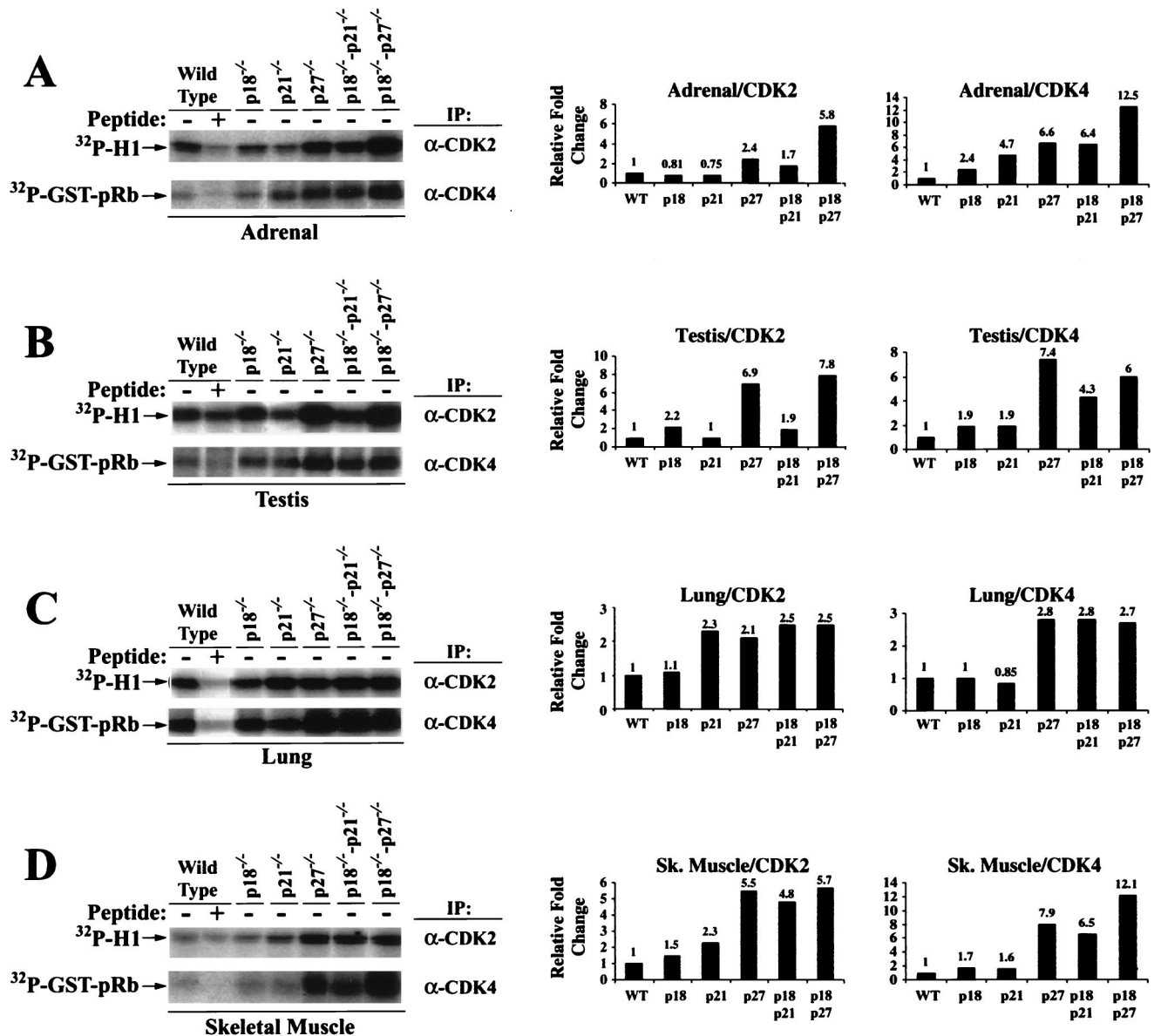
FIG. 6. Loss of CDK inhibitors increases CDK kinase activity. Cell lysates were prepared from adrenal (A), testis (B), lung (C), and skeletal (sk.) muscle (D) obtained from 3-month-old mice of the indicated genotypes. Equal amounts of lysate were immunoprecipitated (IP) with either anti-CDK2 or anti-CDK4 antiserum as indicated. Competing peptides were added to the immunoprecipitations to confirm antibody specificity. Immunocomplexes were assayed for kinase activity using histone H1 (for CDK2) or GST-pRb^{C137} (for CDK4) as substrates. Autoradiographs of the kinase assays are shown on the left. Incorporation of ^{32}P was quantitated, and relative fold change in kinase activity is graphed on the right.

pression function in vivo, yet mice lacking p21 are free of tumor growth (6). Our results provide the first genetic evidence supporting a role of p21 in tumor suppression and an explanation—functional redundancy with another CDK inhibitor gene—for the lack of tumor growth in p21 single mutant mice. It will be interesting to determine the tumor incidence and spectra of mice lacking p21 and other CDK inhibitor genes, especially the members of the INK4 family.

Notably, five of the seven tumors in p18-p27 double mutant mice (pituitary adenoma, adrenal pheochromocytoma, thyroid C-cell adenoma, parathyroid adenoma, and testis interstitial cell adenoma), as well as the pancreatic islet cell hyperplasia, develop in endocrine tissues. This tumor spectrum overlaps in the same cell types as seen in human patients with MEN

syndromes (the combined MEN1 and MEN2 tumor spectra). MEN syndromes refer to a group of diseases characterized by the concurrent development of multiple endocrine tumors and are clinically divided into two major subtypes, MEN1 (pituitary, parathyroid, and pancreatic tumors) and MEN2 (medullary thyroid C-cell carcinomas, pheochromocytomas, and parathyroid tumors), based on their unique combinations of affected endocrine organs (4, 29). All five endocrine organs that are affected in MEN patients exhibit neoplastic or hyperplastic phenotypes in the p18-p27 mutant mice. In addition, like MEN patients, all of the p18-p27 double null animals possessed multiple endocrine tumors (Table 1). It should be pointed out, however, that there are distinct differences between the p18-p27 mutant mice and MEN patients, particu-

larly with nonendocrine pathology. Additional MEN1 pathology includes foregut carcinoids, facial angiofibromas, and multiple lipomatous tumors. MEN2B patients present additional pathology, including hyperplasia of the intrinsic autonomic ganglia in the wall of the intestine, disorganized growth of peripheral nerve axons in the lips, oral mucosa, and conjunctiva, and developmental musculoskeletal abnormalities (e.g., pes cavus, slipped femoral epiphyses, pectus excavatum, and bifid ribs). These abnormalities were not detected in the p18-p27 mutant mice. Likewise, the hyperplasia and tumors of testis Leydig cells and gastrointestinal tumors detected in the p18-p27 mice are not found in MEN patients. The molecular mechanism underlying potential pathological similarities between p18-p27 mutant mice and MEN patients is not clear. It is tempting to speculate that p18 and p27 may interact functionally with the MEN1 tumor suppressor gene product, menin, and/or the c-*RET* proto-oncogene, two genes consistently mutated in MEN1 and MEN2 patients, respectively. While human MEN syndromes can be clinically separated into two major subtypes based on the affected endocrine organs, a division of phenotypes cannot be correlated with different p18-p27 genotypes. Further genetic and biochemical analysis is necessary to establish a regulatory role, if any exists, for either menin or c-Ret in controlling p18 and/or p27 function.

Like p18-p27 double mutant mice, Rb heterozygous mice developed neoplastic phenotypes in multiple endocrine tissues, including the pituitary, thyroid, parathyroid, and adrenal glands (24), providing genetic evidence that p18 and p27 genes function to suppress tumor growth by regulating Rb's tumor suppression function. The p18-p27 and Rb mutant mice exhibit a tumor spectrum completely different from that seen in mice lacking either p53 (7, 13, 30) or its upstream regulators ATM (1, 39) and ARF (18), which develop predominantly lymphomas and soft tissue sarcomas. The molecular basis for such dramatic differences in tumor spectrum between mice lacking genes in the Rb and p53 pathways is not yet understood but may be related to different roles of the Rb and p53 pathways in tumor suppression. p53 functions primarily as a checkpoint gene to monitor genomic integrity, while the function of Rb is to integrate mitogenic signals to determine whether a cell is to enter S phase for another round of division or to arrest in G_1. By allowing accumulation of mutations, loss of p53 function would significantly increase the chance of a cell to become tumorigenic, but only if the cell is in the active division cycle. A stable cell cycle arrest would effectively prevent tumor development even if the genomic integrity checkpoint pathway were impaired. Many endocrine tissues are slow growing or contain very few dividing cells and therefore may become more susceptible to tumorigenesis by the inactivation of the Rb pathway resulting from the loss of both p18 and p27. Mice heterozygous for both p53 and Rb developed multiple endocrine tumors with a spectrum similar to those observed in the p18-p27 mice, but more aggressive in growth (14, 37). Together, these data support a greater role for the Rb pathway (including p18, p27, and Rb) in suppressing tumor initiation and for p53 in suppressing tumor progression.

ACKNOWLEDGMENTS

REFERENCES

1. **Barlow, C., S. Hirotsune, R. Paylor, M. Liyanage, M. Eckhaus, F. Collins, Y. Shiloh, J. N. Crawley, T. Ried, D. Tagle, and A. Wynshaw-Boris.** 1996. Atm-deficient mice: a paradigm of ataxia telangiectasia. Cell **86:**159–171.
2. **Benton, L., L.-X. Shan, and M. P. Hardy.** 1995. Differentiation of adult Leydig cells. J. Steroid Biochem. Mol. Biol. **53:**61–68.
3. **Brugarolas, J., C. Chandrasekaran, J. I. Gordon, D. Beach, T. Jacks, and G. J. Hannon.** 1995. Radiation-induced cell cycle arrest compromised by p21 deficiency. Nature **377:**552–557.
4. **Carney, J. A.** 1998. Familial multiple endocrine neoplasia syndromes: components, classification, and nomenclature. J. Intern. Med. **243:**425–432.
5. **Cheng, M., P. Oliver, J. A. Diehl, M. Fero, M. F. Roussel, J. M. Roberts, and C. J. Sherr.** 1999. The p21^{Cip1} and p27^{Kip1} CDK 'inhibitors' are essential activators of cyclin D-dependent kinases in murine fibroblasts. EMBO J. **18:**1571–1583.
6. **Deng, C., P. Zhang, J. W. Harper, S. J. Elledge, and P. Leder.** 1995. Mice lacking p21$^{CIP1/WAF1}$ undergo normal development, but are defective in G1 checkpoint control. Cell **82:**675–684.
7. **Donehower, L. A., M. Harvey, B. L. Slagle, M. J. McArthur, C. A. Montgomery, J. S. Butel, and A. Bradley.** 1992. Mice deficient for p53 are developmentally normal but susceptible to spontaneous tumours. Nature **356:**215–221.
8. **El-Deiry, W. S., T. Tokino, V. E. Velculescu, D. B. Levy, R. Parsons, D. M. Lin, W. E. Mercer, K. W. V. Kinzler, and B. Vogelstein.** 1993. WAF1, a potential mediator of p53 tumor suppression. Cell **75:**817–825.
9. **Fero, M., E. Randel, K. E. Gurley, J. M. Roberts, and C. J. Kemp.** 1998. The murine gene p27^{Kip1} is haplo-insufficient for tumor suppression. Nature **396:**177–180.
10. **Fero, M. L., M. Rivkin, M. Tasch, P. Porter, C. E. Carow, E. Firpo, K. Polyak, L.-H. Tsai, V. Broudy, R. M. Perlmutter, K. Kaushansky, and J. M. Roberts.** 1996. A syndrome of multiorgan hyperplasia with features of gigantism, tumorigenesis, and female sterility in p27^{Kip1}-deficient mice. Cell **85:**733–744.
11. **Franklin, D. S., V. L. Godfrey, H. Lee, G. I. Kovalev, R. Schoonhoven, S. Chen-Kiang, L. Su, and Y. Xiong.** 1998. CDK inhibitors p18^{INK4c} and p27^{KIP1} mediate two separate pathways to collaboratively suppress pituitary tumorigenesis. Genes Dev. **12:**2899–2911.
12. **Franklin, D. S., and Y. Xiong.** 1996. Induction of p18^{INK4c} and its predominant association with CDK4 and CDK6 during myogenic differentiation. Mol. Biol. Cell **7:**1587–1599.
13. **Harvey, M., M. J. McArthur, C. S. Montgomery, A. Butel, A. Bradley, and L. A. Donehower.** 1993. Spontaneous and carcinogen-induced tumorigenesis in p53-deficient mice. Nat. Genet. **5:**225–229.
14. **Harvey, M., H. Vogel, E. Y.-H. P. Lee, A. Bradley, and L. A. Donehower.** 1995. Mice deficient in both p53 and Rb develop tumors primarily of endocrine origin. Oncogene **55:**1146–1151.
15. **Hedger, M. P., and E. M. Eddy.** 1986. Monoclonal antibodies against rat Leydig cell surface antigen. Biol. Reprod. **35:**1309–1319.
16. **Jenkins, C. W., and Y. Xiong.** 1995. Immunoprecipitation and immunoblotting in cell cycle studies, p. 250–263. *In* M. Pagano (ed.), Cell cycle: material and methods. Springer-Verlag, New York, N.Y.
17. **Kamb, A., N. A. Gruis, J. Weaver-Feldhaus, Q. Liu, K. Harshman, S. V. Tavitgian, E. Stockert, R. S. Day, B. E. Johnson, and M. H. Skolnick.** 1994. A cell cycle regulator potentially involved in genesis of many tumor types. Science **264:**436–440.
18. **Kamijo, T., F. Zindy, M. F. Roussel, D. E. Quelle, J. R. Downing, R. A. Ashmun, G. Grosveld, and C. J. Sherr.** 1997. Tumor suppression at the mouse INK4a locus mediated by the alternative reading frame product p19^{ARF}. Cell **91:**649–659.
19. **Kiyokawa, H., R. D. Kineman, K. O. Manova-Todorova, V. C. Soares, E. S. Hoffman, M. Ono, D. Khanam, A. C. Hayday, L. A. Frohman, and A. Koff.** 1996. Enhanced growth of mice lacking the cyclin-dependent kinase inhibitor function of p27^{Kip1}. Cell **85:**721–732.
20. **Lammie, G. A., and G. Peters.** 1991. Chromosome 11q13 abnormalities in human cancer. Cancer Cells **3:**413–420.
21. **Levine, A. J.** 1997. p53, the cellular gatekeeper for growth and division. Cell **88:**323–331.
22. **Lundgren, K., R. M. de Oca Luna, Y. B. McNeill, E. P. Emerick, B. Spencer, C. R. Barfield, G. Lozaano, M. Rosenberg, and C. A. Finlay.** 1997. Targeted expression of MDM2 uncouples S phase from mitosis and inhibits mammary gland development independent of p53. Genes Dev. **11:**714–725.
23. **Nakayama, K., N. Ishida, M. Shirane, A. Inomata, T. Inoue, N. Shishido, I. Horii, D. Y. Loh, and K.-I. Nakayama.** 1996. Mice lacking p27^{Kip1} display increased body size, multiple organ hyperplasia, retinal dysplasia, and pituitary tumors. Cell **85:**707–720.
24. **Nikitin, A. Y., M. I. Juarez-Perez, S. Li, L. Huang, and W.-H. Lee.** 1999. RB-mediated suppression of spontaneous multiple neuroendocrine neopla-

sia and lung metastases in Rb$^{+/-}$ mice. Proc. Natl. Acad. Sci. USA **96:**3916–3921.

25. **Nobori, T., K. Mlura, D. J. Wu, A. Lois, K. Takabayashi, and D. A. Carson.** 1994. Deletion of the cyclin-dependent kinase-4 inhibitor gene in multiple human cancers. Nature **368:**753–756.

26. **Oliner, J. D., K. W. Kinzler, P. S. Meltzer, D. L. George, and B. Vogelstein.** 1992. Amplification of a gene encoding a p53-associated protein in human sarcomas. Nature **358:**80–83.

27. **Park, M., J. Rosai, H. T. Nguyen, P. Capodieci, C. Cordon-Cardo, and A. Koff.** 1999. p27 and Rb are on overlapping pathways suppressing tumorigenesis in mice. Proc. Natl. Acad. Sci. USA **96:**6382–6387.

28. **Phelps, D., and Y. Xiong.** 1997. Assay for cyclin D-dependent kinases 4 and 6. Methods Enzymol. **283:**194–205.

29. **Ponder, B. A., and D. Smith.** 1996. The MEN II syndromes and the role of the ret proto-oncogene. Adv. Cancer Res. **70:**179–222.

30. **Purdie, C. A., D. J. Harrison, A. Peter, L. Dobbie, S. White, S. E. M. Howie, D. M. Salter, C. C. Bird, A. H. Wyllie, M. L. Hooper, and A. R. Clarke.** 1994. Tumor incidence, spectrum and ploidy in mice with a large deletion in the p53 gene. Oncogene **9:**603–609.

31. **Serrano, M., H.-W. Lee, L. Chin, C. Cordon-Cardos, D. Beach, and R. A. DePinho.** 1996. Role of the INK4a locus in tumor suppression and cell mortality. Cell **85:**27–37.

32. **Sherr, C. J.** 1996. Cancer cell cycle. Science **274:**1672–1677.

33. **Sherr, C. J.** 1998. Tumor surveillance via the ARF-p53 pathway. Genes Dev. **12:**2984–2991.

34. **Song, W. C., Y. Qian, X. Sun, and M. Negishi.** 1997. Cellular localization and regulation of expression of testicular estrogen sulfotransferase. Endocrinology **138:**5006–5012.

35. **Wang, T. C., R. D. Cardiff, L. Zukerberg, E. Lees, A. Arnold, and E. V. Schmidt.** 1994. Mammary hyperplasia and carcinoma in MMTV-cyclin D1 transgenic mice. Nature **369:**669–671.

36. **Weinberg, R. A.** 1995. The retinoblastoma protein and cell cycle control. Cell **81:**323–330.

37. **Williams, B. O., L. Remington, D. M. Albert, S. Mukai, R. T. Bronson, and T. Jacks.** 1994. Cooperative tumorigenic effects of germline mutations in *Rb* and *p53*. Nat. Genet. **7:**480–484.

38. **Xiong, Y., H. Zhang, and D. Beach.** 1993. Subunit rearrangement of cyclin-dependent kinases is associated with cellular transformation. Genes Dev. **7:**1572–1583.

39. **Xu, Y., T. Ashley, E. E. Brainerd, R. T. Bronson, M. S. Meyn, and D. Baltimore.** 1996. Targeted disruption of ATM leads to growth retardation, chromosomal fragmentation during meiosis, immune defects, and thymic lymphoma. Genes Dev. **10:**2411–2422.

40. **Yan, Y., J. Frisen, M.-H. Lee, J. Massague, and M. Barbacid.** 1997. Ablation of the CDK inhibitor p57^{Kip1} results in increased apotosis and delayed differentiation during mouse development. Genes Dev. **11:**973–983.

41. **Zhang, P., N. Liegeois, C. Wong, M. Finegold, H. Hou, J. C. Thompson, A. Silverman, J. W. Harper, R. A. DePinho, and S. J. Elledge.** 1997. Altered cell differentiation and proliferation in mice lacking p57^{KIP2} indicates a role in Beckwith-Wiedemann syndrome. Nature **387:**151–158.

42. **Zhang, P., C. Wong, R. A. DePinho, J. W. Harper, and S. J. Elledge.** 1998. Cooperation between the Cdk inhibitors p27^{KIP1} and p57^{KIP2} in the control of tissue growth and development. Genes Dev. **12:**3162–3167.

43. **Zhang, P., C. Wong, D. Liu, M. Finegold, W. Harper, and S. J. Elledge.** 1999. p21^{CIP1} and p57^{KIP2} control muscle differentiation at the myogenin step. Genes Dev. **13:**213–224.